TEM study of carbon nanoparticles. Relationships multiscale organization - properties

Jean-Noël Rouzaud[1], Stanislaw Duber[2], Miroslawa Pawlyta[2],
Thomas Cacciaguerra[3], Christian Clinard[3]

1. Laboratoire de Géologie, Ecole Nationale Supérieure (ENS) de Paris
24, rue Lhomond, 75005-PARIS Cedex. France
2. Faculty of Earth Sciences, University of Silesia,
41-200 Sosnowiec, ul. Bedzinska 60, Poland
3. Centre de Recherche sur la Matière Divisée, CNRS-Université d'Orléans
1B, rue de la Férollerie 45071-Orléans Cédex 2 France

Corresponding author : rouzaud@geologie.ens.fr

Introduction

Carbon nanoparticles, as carbon blacks and soot, are very dispersed polyaromatic solids, of nanometric size, resulting from pyrolysis or partial combustion of liquid or gaseous hydrocarbons [1]. Soot are from natural origin (forest fires) or anthropic ones (fossil fuel combustion, internal combustion engines). They are suspected to play a noticeable effect on air pollution and could be involved in green house effects and subsequent possible climatic changes. Different ways are used by car industry either to limit their production, to trap the soot in filters, or to destroy them by a post-combustion process, usually assisted with a catalyst. Such carbon nanoparticles are characterized by a multiscale organization (structure, microtexture, texture). It can be directly imaged by High Resolution Transmission Electron Microscopy (HRTEM) over than 3 orders of magnitude (µm-nm) [2,3]. In order to access to quantitative data, analysis of HRTEM images is required and was recently developed [4-7]. Relationships can be thus obtained between precursor nature, conditions of formation, multiscale organization and properties such as reactivity or light absorption [8]. The multi-scale organization appears thus to be a fingerprint of the formation of these disordered and divided carbons. After studies on soot from laser pyrolysis [6], shock tube device [8] and from diesel engines, this paper is focused on a series of commercial carbon blacks. Relationships between multiscale organization and reactivity in air-combustion at 800°C were studied to simulate soot destruction by an oxidative post-treatment. First data on reflectance of soot are also presented.

Experimental

Sampling. The conditions of formation of soot in the tube shock device are much more mastered than in diesel engine. However, the available quantity being only few milligrams, it is impossible to perform reactivity tests and optical measurements. Consequently, we chose here a series of five reference black carbon samples, with very different characteristics (see table 1) to obtain a sampling representative of the variety of the engine soot, with expected different organizations and reactivities. BET

measurements were obtained by the NOVA 2200 (Quantachrome) device. Samples were previously out-gassed in a vacuum at 300 °C for ca 18 h. All computations were performed for dry samples. For the measurement of the particle diameter, electron micrographs were obtained by the transmission electron microscope Philips EM 400 with a magnification of 50,000 x (see below). Table 1 shows our sampling gathers very different characteristics, especially as far as S_{BET} is concerned (from 51 m^2/g for Printex 25 up to 1003 m^2/g for Printex XE2B).

Samples	S_{BET} (m^2/g)	V_{total} [cm^3/g]	Particle Diameter (nm)	Fractal Dimension D_{peri}
Printex XE2B	1003	1,221	18.2	1.67
FW 200	545	0,718	9.6	1.72
Printex 90	336	0,604	7.9	Nd
Printex 60	106	0,148	17.8	nd
Printex 25	51	0,079	25.7	1.45

Table 1. Some characteristics of the studied carbon blacks

Characterization of the multiscale organization. Carbon blacks are made of more or less ramified chains of round shape nanometric particles forming more or less closed submicrometric aggregates. The particles usually show a more or less developed concentric microtexture and a turbostratic structure [2,3,7].

Structural data. Whereas X-ray Diffraction (XRD) and spectroscopic method (as NMR) usually give only averaged structural data, HRTEM allows to image it directly over about three orders of magnitude (0.3 to 300 nm). The sphere size was determined on medium magnification images (50,000 x), whereas structural data were extracted from high resolution images (resolution better than 0.15 nm with the Philips CM20 used here). Thanks to an original home-made method of image analysis we specifically developed for such divided carbons, quantitative de-averaged structural data can be obtained [5,6]. After skeletonization of the raw images obtained at 310,000 x, our software allows to analyze each fringe individually and in relation with its neighbors and to specify the boundaries of coherent domains and the proportion of non-stacked layers. De-averaged structural data can then be extracted, giving the distributions of : L the fringe length (i.e. the polyaromatic layer extent), d_{002} the interlayer spacings, Lc and La the height and the diameter of the coherent domains respectively, and N the number of stacked layers forming a coherent domain [5]. The errors on the measurements can be estimated here to be lower than +/- 0.05 nm.

Textural data. Medium magnification (50,000x) TEM images (Figure 1) were used to access to information on the organization at the texture scale (about 10 nm - 1 µm range). The micrographs are scanned and analysed by the image analyser. For each sample, the diameters of more than 200 particles are measured to calculate the average particle diameter of the sample. According to the sample, the mean size of the spherules (and the ramification degree of the chains) change (see table 1), as already observed for the shock tube soot where the spherule size decreases with the temperature of formation, whereas the compactness of the aggregates increases [8].

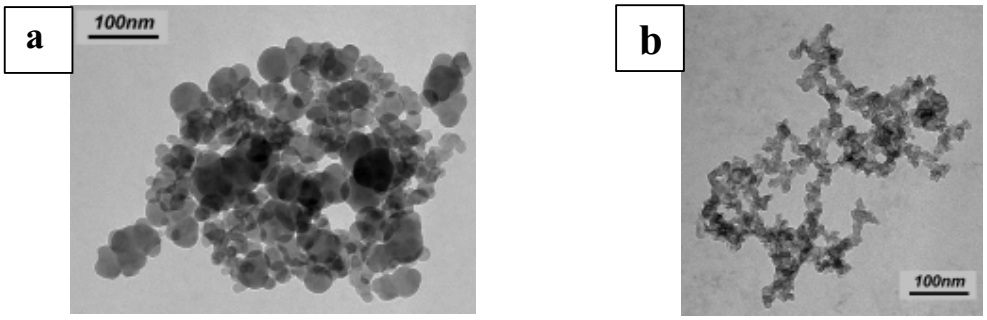

Figure 1. Medium magnification TEM images of Printex 25 (a) and Printex XE 2B (b)

The Printex 25 (Figure 1a) sample exhibits the largest spherules (up to 80 nm), whereas the FW200 sample the smallest ones (about 20 nm). The size of the latter is similar to the soot synthesized by the shock tube device [8], whereas that of the Printex 25 appears significantly larger. Several methods were tested in order to obtain the fractal dimension of soot aggregates [9]. The fractal dimension of the particle counting method needs to specify the particle number per aggregate in the TEM micrographs. The compactness of some carbon black aggregates, like Printex 25, makes such determination difficult and calculations inaccurate. By contrast, in the method of the peripheral fractal dimension (D_{peri}), the knowledge of the particle number per aggregate are not necessary. Thanks to this method, Hayashi et al. [10] found that commercial carbon blacks have various values of D_{peri}. They show that parameter D_{peri} may be effective as an index to evaluate the fractal properties of soot.The peripheral fractal dimension, $D_{peri,}$ is expressed by:

$$P \propto A_p^{\frac{D_{peri}}{2}}$$

where P is perimeter of an aggregate and A_p is the projected area of an aggregate in the TEM micrographs. is obtained as a slope from A_p versus P in log-log plot. Fractal dimensions of our carbon blacks, determined by the measurement of D_{peri} are gathered in table 1 [9]. Aggregates with compact structure have smaller D_{peri} value than aggregates with open structure and higher surface, because this parameter is a measure of the ruggedness of the boundary. For instance, D_{peri} is 1.45 for the Printex 25 (see figure 1a), whereas it is 1.67 for XE-2B (see figure 1b).

HRTEM structural characterization Characteristic high magnification and high resolution TEM images are given in the Figures 2 and 3. The Printex 25 (Figures 2) is clearly the most ordered : the concentric microtexture is well developed and the spherule size is the largest (about 80 nm). It must be noticed that the spherules are strongly packed and partial spherule coalescence can be observed. Consequently this sample is characterized by compact aggregates of large and weakly accessible particles.

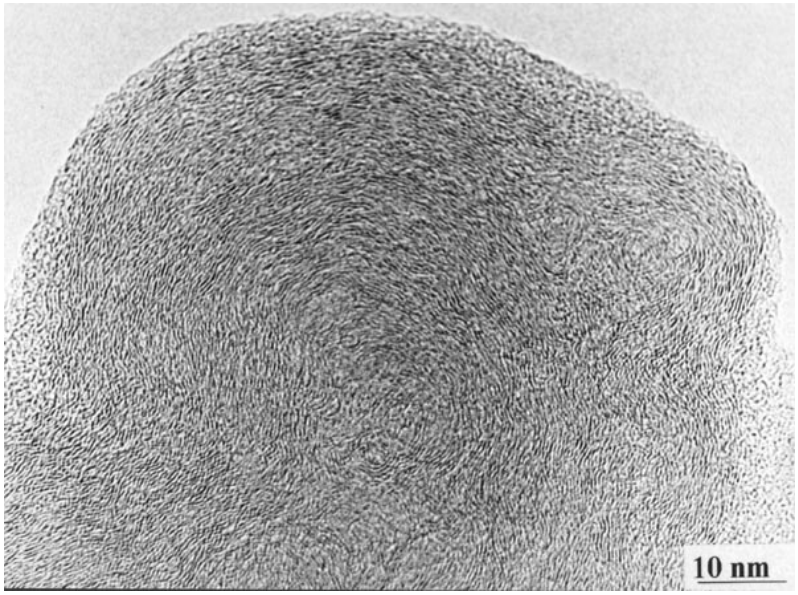

Figure 2. HRTEM images of the Printex 25 black carbon

By contrast, the FW 200 sample (Figure 3) shows the smallest spherules (about 20 nm) and the concentric microtexture is here less developed (the layers are short and weakly stacked). The XE-2B sample appears more complex : even though the spherules (about 30 nm in diameter) are sensibly more distinguishable, the concentric microtexture is poorly expressed, the spherules; more longer layers (up to 1 nm) on the external parts of the spherules coexists with smaller ones on the internal part.
Such information shows that TEM data are in a good agreement with BET ones.

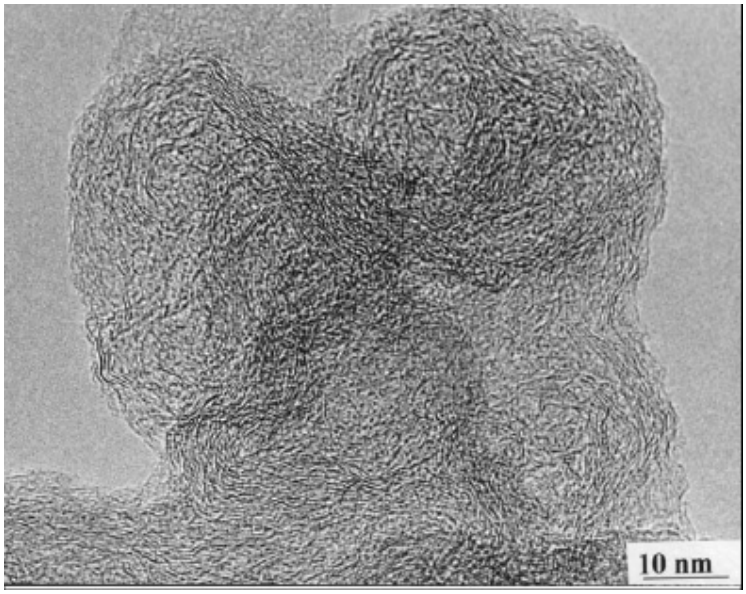

Figure 3 HRTEM images of FW 200.

The mean structural parameters obtained from image analysis are gathered in table 2.

SAMPLE	L nm	NSL %	d_{002} nm	La nm	Lc nm	N
PRINTEX 25	0.76	34	0.41	0.53	0.76	2.9
PRINTEX 90	0.60	54	0.42	0.41	0.65	2.6
PRINTEX 60	0.56	61	0.45	0.38	0.58	2.3
FW200	0.57	67	0.44	0.37	0.62	2.4
XE-2B	0.55	68	0.45	0.42	0.62	2.4

Table 2. Structural parameters measured by HRTEM image analysis

These measurements strengthen the visual observations and give quantitative data required for a better interpretation of the soot properties. As far as the averaged values are discussed, the Printex 25 sample is the most ordered : largest layers (0.76 nm), smallest amounts of non-stacked layers (NSL) (34 %), smaller interlayer spacings (0.41 nm), largest coherent domains (largest La and Lc), and greatest number of stacked layers (2.9). By contrast, the FW200 and XE-2B samples are the less organized, as shown by their small layer extent (less than 0.6 nm), the high proportion of single layers (about 70 %) and their large interlayer spacings (0.44-0.45 nm). Distribution of each parameter allows to access to de-averaged data; histogram of the layer extent is given as an example in the Figure 4.

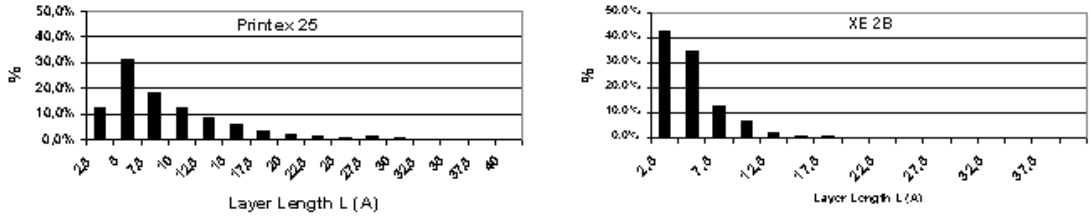

Figure 4. Histograms of layer extent, as measured by HRTEM image analysis, on Printex 25 (a) and XE-2B (b) black carbons.

Oxyreactivity data. Measurements of oxyreactivity were performed by using thermogravymetry method. Each analyzed carbon black sample was burnt using a thermal balance (MOM Budapest, F. Paulik, J. Paulik, L. Erdey system). 80 mg samples were prepared by blending carbon black and Al_2O_3 (previously dried in air at 1100 ^oC) in 1:3 ratio and were carefully mechanically mixed during 15 minutes. Each samples were submitted to thermogravymetry (TG) as well as differential thermal analysis (DTG) over the temperature range from ambient to 800 ^oC, at a heating rate of 10 ^oC/min in dry air flow of ca 1 dm^3/min. The DTG curves are gathered on the Figure 5.

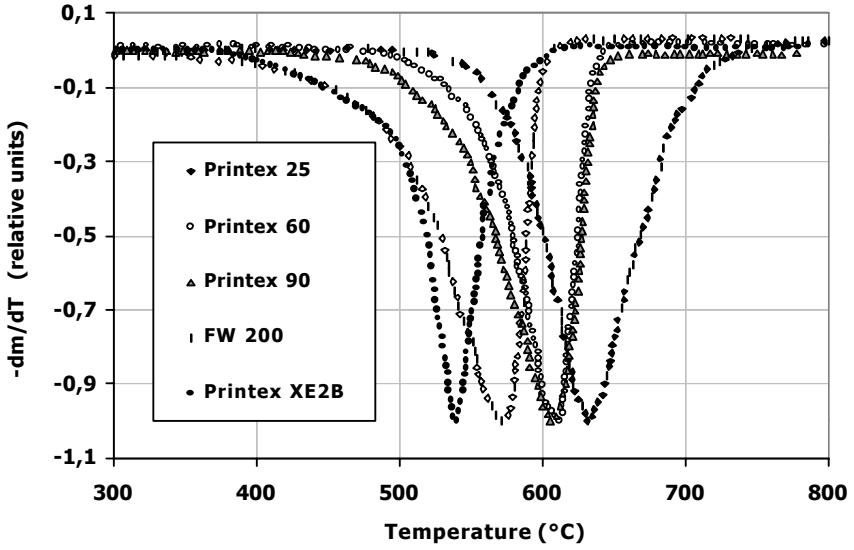

Figure 5. DTG curves of the 5 carbon black samples studied here

These samples show different behaviors. As far as the multiscale organization is concerned, the Printex 25 sample appears as the less reactive, since a temperature of more than 700°C is required for the complete destruction of these carbon blacks, the maximum rate of oxidation occurring at about 630°C. By contrast, the FW 200 and XE-2B samples are the most reactive, since they are completely burnt at a much lower temperature (about 600°C), the maximum rate of oxidation occurring at about 550°C. The behavior of the Printex 90 and the Printex 60 samples are very similar and intermediate between the two previously described poles. A global relationship was found between the reactivity and the BET surface area (Figure 6).

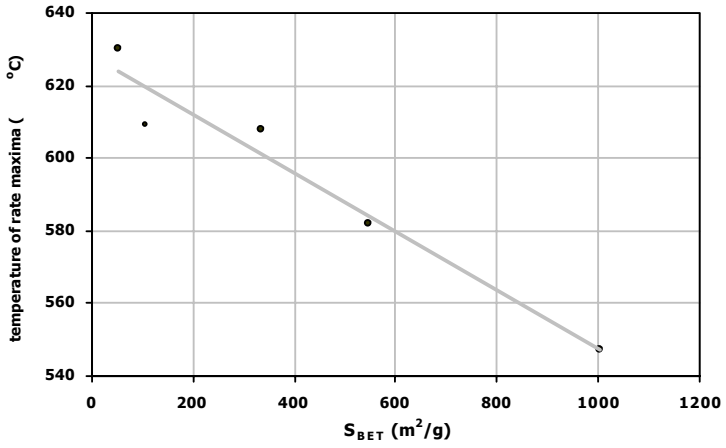

Figure 6. Temperature of rate maxima versus S_{BET} for the five carbon blacks studied here

However, the multi-scale organization HRTEM quantitative data could allow a better understanding of these reactivity results. For instance, a good correlation appears between the black carbon reactivity and the layer extent L (compare Figures 2, 3, 4, and Table 2). This confirms results previously obtained on carboxyreactivity of cokes [11,12]. Moreover, significant differences appear in the shape reactivity curves: some of them exhibit a rather symmetric V shape (XE-2B and Printex 25), whereas the decrease of the reactivity rate after the maximum is more abrupt for the 3 other samples. The smallest and the most distorted accessible layers are probably burnt first, and the longest and straightest ones the last [13]. This could explain the behavior of the XE-2B sample, formed by numerous small layers (40% of the layers are 0.25 to 0.5 nm length) coated by an external part formed by noticeably longer layers. By contrast, the large spherules of the Printex 25 are partially coalesced, deleting the oxygen accessibility to the edge of the polyaromatic planes; the layers are larger (only 10 % of the layers are 0.25 to 0.5 nm length, and the largest extent can reach 3 nm) responsible for a rather broad layer extent distribution); this could explain the symmetric shape of its reactivity curve. However, up to now, no really satisfying explanation was found. The role of defects, responsible for layer distortion has probably to be taken into account, since such defects are preferential sites for oxygen reaction. Moreover, the reactivity depends also on the accessibility of the spherules to oxygen. This accessibility, connected to the compactness of the aggregates, i.e. on their fractal dimension, has to be specified.

First reflectance measurements

Reflectance of carbon blacks was determined on pressed powders using polarized light (l = 545 nm). The values given in the table correspond to the average calculated on more than 100 measurements. As expected on the basis of optical properties of other carbons [13-15], the better the degree of organization, the higher the reflectance. The highest reflectance is thus obtained with the Printex 25 black carbons, characterized by the most improved structural (largest layers and coherent domains, smallest amounts of non-stacked layers, smaller interlayer spacings) and the lowest for the XE-2B black carbons which are the most disordered carbons of this series. Apparently surprising high reflectance is obtained with the FW 200 black carbons. However, these blacks were obtained in oxidizing conditions. It is known that oxidation of carbons is responsible for an reflectance increase [16].

Samples	Reflectance in air (%)	Standard Deviation (%)
Printex XE-2B	2.46	0.68
FW 200	7.04	1.04
Printex 90	5.28	0.55
Printex 60	4.14	0.79
Printex 25	8.43	0.81

Table 3. Reflectance of the carbon blacks studied here

The measurements of reflectance in a second immersion medium (oil is classically chosen) will allow to calculate the real and the imaginary part of the complex refractive index [16]. Realistic values could be then obtained for such disordered and divided carbons. Up to now, in the calculations of transmittance and reflectance, they are usually chosen constant and close to the graphite values, whereas these optical parameters of the carbon change according to their organization [15]. Moreover, this rises some doubts on the reliability of simulations of the measurement of the soot yield in the shock tube by the classical method of laser extinction [8]. Such precise measurements of light absorption and reflection of light on atmospheric aerosols could allow to specify a possible role of carbon nanoparticles on the green house effect and subsequent climatic changes.

Conclusion

Commercial black carbons were chosen as reference samples of diesel soot, since available in sufficient quantity to perform reactivity test. A series of 5 black carbon commercial samples was selected on the basis of their strongly different BET surface areas. This study shows demonstrate that various textures, microtextures and structures can be obtained depending on the conditions of soot or carbon black formation. A quantitative knowledge of the multiscale organisation of the soot allows a better expectation of their properties (reactivity, optics). An interesting relationship was found between BET surface area and explain the oxyreactivity; this could allow a better forecast of the effect of combustion post-treatments for de-sooting. However, behavior of the carbon blacks during their oxidation remains to be completely interpreted. A first meaningful relation was found with the layer extent L, as measured by image analysis from HRTEM images. Complementary image analysis (layer distortion, fractal dimension of the aggregates) are required on the raw and on the partially burnt samples. Extrapolation of these data to the destruction of “real” soot from diesel engines, has now to be tested and discussed.

References

[1] J.B. Donnet, R.C. Bansal, and M.J. Wang Eds, Carbon black Science and Technology, Marcel Dekker, New-York, 1993, 2nd edition.
[2] Heidenreich RD, Hess, WH and Ban LL.A test object and criteria for high resolution microscopy. J. Appl. Cryst., 1 (1968), 1-18.
[3] Oberlin, Agnès. “High Resolution TEM studies of carbonization and graphitization”. In *Chemistry and physics of carbon*, Vol 22, Thrower P.A. (Ed.), Marcel Dekker, New-York, 1989, p. 1-143.
[4] Shim H.S., Hurt R.H. and Yang N.Y.C. A methodology for analysis of 002 lattice fringe images and its application to combustion-derived carbons. Carbon 2000; 38:29-45
[5] J.N. Rouzaud and C. Clinard. Quantitative High Resolution Transmission Electron Microscopy : A Promising Tool for Carbon Materials Characterization. Fuel Processing Technology, 77-78 (2002), 229-235.
[6] A. Galvez, N. Herlin, C. Reynaud, M. Cauchetier and J.N. Rouzaud. Nanoparticles produced by laser pyrolysis of hydrocarbon, Carbon 40 (2002), 2775-2789.

[7] R.L. Rander Wal, A.J. Tomasek, K. Street, D.R. Hull and W.K. Thompson. Carbon Nanostructure Examined by Lattice Fringe Analysis of Transmission Electron Microscopy Images, Applied Spectroscopy 58 (2004), 230-237.
[8]. F. Douce, N. Djebaï li-Chaumeix, C. Paillard, C. Clinard and J.N. Rouzaud (2000). Carbon nanoparticles formation during the pyrolysis of heavy hydrocarbons behind shock waves. Extended Abstracts Intern. Conf. Carbon 2000, Berlin, 9-14 juillet 2000, 1063-1064.
[9] S. Duber and, M. Pawlyta. Fractal properties of soot aggregates. In : « Matériaux carbonés et catalytiques pour lenvironnement. Extended Abstracts, Zakopane Sept. 25-30 2003, pp 187-193.
[10] S. Hayashi, Y. Hisaeda, Y. Asakuma, H. Aoki, T. Miura, H. Yano, Y. Sawa (1999). Simulation of Soot Aggregates Formed by Benzene Pyrolysis. Combustion and Flame 117:851–860
[11] J.N. Rouzaud, B. Duval and J. Leroy. Coke microtexture : a key for coke reactivity. In "Fundamental Issues in Control of Carbon Gasification Reactivity", 1991, J. Lahaye and P. Ehrburger Eds., Kluwer Academic Publisher, 257-268.
[12] C. Monéger, F. Béguin and J.N. Rouzaud. Carboxyreactivity of carbons : a structural and microtextural approach. Ext. Abstracts. Eurocarbon 98, Strasbourg, 5-9 juillet 1998, 149-150.
[13] S. Duber, J.N. Rouzaud, C. Clinard and S. Pusz. Microporosity and optical properties of some activated chars. Fuel Processing Technology, 77-78 (2002), 221-227.
[14] J.N. Rouzaud and A. Oberlin. Structure, microtexture and optical properties of anthracene and saccharose-based carbons. Carbon, 1989, 27, 517-529.
[15] J.N. Rouzaud, A. Oberlin & C. Bény-Bassez (1983). Carbon films: structure and microtexture (optical and electron microscopy, Raman spectroscopy). Thin Solid Films, 105, 75-96.
[16] D.W. Van Krevelen. *Coal*. Elsevier, Amsterdam, 1961.